

Characterizing the Nonequilibrium Response of FeRh Thin Films using Time-Domain Thermoreflectance (TDTR)

Renee M. Harton,^{1,*} Alejandro Ceballos,² and Frances Hellman²

¹*University of Illinois at Urbana-Champaign
Department of Materials Science and Engineering,
1304 W Green St, Urbana, IL 61801*

²*Department of Physics, University of California,
366 Physics North Berkeley, CA, 94720-7300, USA*

(Dated: December 7, 2022)

Abstract

Two-tint Time-Domain Thermoreflectance (TDTR) characterization of FeRh throughout its first order antiferromagnetic (AF) to ferromagnetic (FM) transition shows that the transient reflectance, $\Delta R(t)/R$, strongly depends on the magnetic order of the sample. Using a probe wavelength of approximately 783 nm, we have found that the $\Delta R(t)/R$ of the AF phase exhibits a large negative response, while the response of the FM phase is positive. This magnetic phase sensitivity has allowed us to study the transient response of both the AF and FM phase to the pump pulse excitation as well as the mixed phase of the material. We have found that the AF phase exhibits a strong transient signal which is not observed in the FM phase. A model using linear system techniques was able to represent and analyze the behavior of the system in each phase. The thermalization time of the electrons in the AF phase occurred on a timescale at least twice as long as that in the FM phase. These results indicate that the two-tint TDTR can be used to study the transient properties of the AF and FM phase of FeRh as well as the mixed phase.

I. INTRODUCTION

Iron-rhodium alloys, $\text{Fe}_x\text{Rh}_{1-x}$, with Fe compositions, x , between $0.48 < x < 0.52$, exhibit a first-order magnetic phase transition near room temperature.¹ Although this phase transition was first observed by Fallot et al. in 1938,² it has long been investigated by researchers due to its advantageous properties such as large magnetoresistance³ and magnetostriction.⁴ In addition, its proposed technological applications, for example, heat-assisted magnetic recording are of interest.^{5,6} This attention has resulted in a rich body of research focused on the structural and magnetic properties of FeRh alloys.

The magnetic phase transition occurs across a range of temperatures and exhibits hysteresis which is dependent on both composition and microstructure.^{7,8} For temperatures below the transition, the magnetic order of the material is antiferromagnetic (AF); above the transition region, the material is ferromagnetic (FM). For temperatures within the AF/FM transition region, the sample exhibits a mixed phase of AF and FM domains.^{9,10} Near and throughout the transition region, FeRh exhibits CsCl crystalline structure; as the sample

* hartonr22@gmail.com

undergoes the AF/FM transition with increasing temperature, the lattice constant increases by $\approx 0.1\%$.¹¹

The intriguing nature of the FeRh AF/FM transition has motivated researchers to investigate its origin and to thoroughly examine the different properties of the AF and FM phases, these studies have led to a thorough exploration of the different properties of the AF and FM phase of FeRh. First principle calculations using density functional theory show that the density of states (DOS) of the AF phase exhibits a pseudogap of approximately 0.5 eV near the Fermi energy.¹² For the FM domains, this pseudogap is not observed. These results are supported by Hall effect measurements which determine that the Hall coefficient decreases by almost an order of magnitude as the number and size of the FM domains grows with an increase in temperature in the transition region.¹³ The source of this difference in Hall coefficient is an increase in the carrier density concomitant with an increase in the density of states near the Fermi energy in the FM phase relative to the AF phase. Another experimental result supporting the pseudogap of the AF phase was found by Pressacco et al.¹⁴ Using X-Ray Photoemission Spectroscopy, Pressacco et al. demonstrated an increase in the electron spectral weight with the formation of FM domains. These results show that as the FM phase grows in size with an increase in the base temperature of the sample, the density of states near the Fermi energy also increases. One might wonder how the presence of the pseudogap in the AF phase and the absence of this feature in the FM phase affects the response of FeRh to an optical pump pulse.

The response of FeRh to optical pump pulse excitation has intrigued researchers for decades. Pump-probe techniques, such as Time-Resolved Magneto-Optic Kerr Effect (TR-MOKE) magnetometry, Time-Resolved x-ray diffraction, and Time-Resolved photoelectron spectroscopy have been used to study the transient response of FeRh. From these studies, the onset of FM order has been observed on both the sub-picosecond^{15,16} and picosecond timescales.^{14,17} As a result, the limiting timescale of the AF/FM transition remains a source of debate.

Although the timescale of the FeRh AF/FM transition has been reported using several detection methods, these measurements used large pump fluences. Moreover for the referenced studies, the pump fluence was systematically increased to induce the transition.^{15,18} These measurements identified a threshold pump fluence required to drive the AF/FM transition. Since the nonequilibrium response of metals depends on pump fluence,¹⁹ it is challenging to

decouple the effects caused by changes in phase fraction from those caused by altering the fluence of the pump. In the studies reported here we used time-domain thermorefectance (TDTR) to determine the response of FeRh thin films to pump excitation. For these measurements, the temperature per pulse of the pump beam was 2K. The width of the AF/FM transition for comparable FeRh films is approximately 70 K.²⁰ Since the temperature per pulse used for this measurement is less than 3% of the width of the AF/FM transition, we were able to study dynamics of FeRh for temperatures within the AF and FM regions as well as throughout the AF/FM transition region.

Although TR-MOKE is able to detect the FM phase, the dynamics of the AF phase have been difficult to measure using these methods. Recently, quadratic MOKE has been used to study the magnetization dynamics of the metallic antiferromagnet, Fe₂As.²¹ The analysis of this method requires that the components of the dielectric function tensor that are linear and quadratic in magnetization are zero. FeRh exhibits a remnant magnetization in the AF phase due to a residual FM component and a mixed phase throughout the AF/FM transition. Thus, the nonequilibrium response of the AF phase of FeRh as well as the response of the mixed phase is difficult to isolate using quadratic MOKE. Our results show that the transient reflectance can be used to detect the sub-picosecond response of AF domains in the transition region when FM domains are present, which to the best of our knowledge cannot be detected using other conventional methods.

Since transient reflectance is commonly used to study the electronic and structural properties of materials on the femtosecond timescale, the transient reflectivity of FeRh across the AF/FM transition has been measured previously.^{15,22} For these measurements, the pump beam consisted of an 800 nm femtosecond pulse train and the probe beam consisted of the second harmonic of this pulse train centered at 400 nm. For these measurements, the pump fluences are comparable to our setup.¹⁸ At these pump and probe frequencies and fluences, the transient reflectance measured did not exhibit a significant dependence on AF/FM phase fraction. As a result, for this pump-probe configuration, the transient reflectance, $\Delta R/R(t)$, was used to deduce the response of the lattice to pump pulse excitation.^{15,22} Since the transient reflectance depends strongly on the probe wavelength,²³ one might consider if it is possible to tune the probe wavelength such that the transient reflectance of FeRh is sensitive to the magnetic phase of the material. This question is the focus of this paper.

For this work, we have used two-tint time-domain thermorefectance to study the nonequi-

librium response of the AF, FM and mixed phases of FeRh. This technique reveals a marked difference in the subpicosecond response of FeRh AF and FM phases. Using the phase-sensitivity of this technique, we have studied the dependence of the system response of FeRh on the relative AF/FM phase fraction for time delays shorter than the thermalization time of the electrons of the system.

The results of this study are significant, because we are able to detect the AF phase on the femtosecond timescale and thus observe how it responds to pump pulse excitation for base temperatures below and throughout the AF/FM transition. Using the same technique, we are then able to compare these results to the response of the FM phase. To analyze these results, we have used linear systems techniques to model the response of the system to pump excitation.

II. EXPERIMENTAL METHODS

For this work, we conducted TDTR measurements on a Pt(3 nm)/Fe₄₉Rh₅₁(19 nm)/MgO(100) sample. The sample compositions were determined using Rutherford backscattering spectrometry. The temperature dependence of the AF/FM transitions of the sample was characterized using a Magnetic Property Measurement System (MPMS).

For the MPMS measurements, the sample was configured such that the applied magnetic field was parallel to the sample plane. To align remnant FM domains in the sample, we applied a magnetic field during the temperature dependent measurements. We determined the required magnitude of the applied field by conducting magnetic field dependent measurements at room temperature. The minimum field needed to overcome the domain pinning energy was 900 Oe. This magnitude was small enough that both the diamagnetic response and the shift in the temperature of the AF/FM transition were negligible.²⁴ The results are displayed in Figure 1.

For the TDTR measurements, a mode-locked Titanium:Sapphire ultrafast laser with a pulse repetition rate of 80 MHz was used. The central wavelength of the generated pulses was set to 783 nm. The pump and probe beams were separated into orthogonal components using a polarizing beamsplitter. The beams were then spectrally separated using a two-tint pump-probe method which employed a 785 nm RazorEdge ultrasteep short-pass edge filter

cutoff frequency of 785 nm for the pump beam and a 785 nm RazorEdge ultrasteep long-pass edge filter for the probe beam.²⁵

For the described measurements, the powers of the pump and probe beams were 7 mW and 3 mW, respectively. These beams were focused onto the sample using a 5x microscope objective lens with a spot size of 10.6 μm . The resultant temperature per pulse of the pump and probe beams were approximately 2 K and 1 K, respectively. The steady state heating of the pump and the probe beams was approximately 1 K and 0.8 K, respectively.

The pump-induced effects on the sample were measured using lock-in detection. The pump beam was modulated at 11 MHz using an electro-optic modulator. Double-modulation was used to reduce the radio-frequency coherent pickup.²⁶ Double-modulation was achieved using a computer-based lock-in audio-frequency detector while the probe beam was modulated at a rate of 200 Hz using a mechanical chopper. The time delay between the pump and probe pulses was achieved by altering the relative path length of the pump and probe beam path using a retroreflector along the pump beam path.

To ensure uniform heating the FeRh sample was mounted onto a $\text{SiO}_2(300 \text{ nm})/\text{Si}$ substrate using Ag paste. Measurements were conducted using an Instec heating and cooling stage to control the base temperature of the sample. We determined the temperature range for the TDTR measurements using the results of the magnetic hysteresis characterization of the sample. The range of base temperatures used for this study was 300 K-410 K. The pump-probe correlation function was determined by a cross-correlation measurement using the pump and the probe beams. For this measurement, we used a Thorlabs DET25K GaP detector.

III. EXPERIMENTAL RESULTS

The magnetic hysteresis of the FeRh sample is displayed in Figure 1. The AF/FM transition can be divided into five phases for increasing and decreasing temperatures. In Region I, the sample is majority AF. Between Region II-Region IV, the sample undergoes the AF/FM transition. For temperatures within Region II and Region IV, the sample employs two mechanisms to undergo the AF/FM transition: nucleation and domain growth.²⁷ In Region II there is an increase in the number of FM domains by nucleation at sites within

the AF background. In Region III, the number of FM domains remains roughly the same while the nucleated FM domains increase in size. The growth of the FM domains is reflected in Figure 1 by the change in the slope of the magnetization with respect to temperature. In Region V, the sample is majority FM. As the temperature is further increased, the magnetization decreases as the sample approaches the Curie temperature of FeRh ($T_C=670$ K). For temperatures below the AF/FM transition (Region I and Region X), the sample consists of a majority of AF domains. However, a remnant magnetization of 59 emu/cm^3 is observed. This nonzero magnetization below the onset of the transition can be explained by residual FM domains which have also been observed in similar FeRh samples.²⁸⁻³⁰ It accounts for approximately 7% of the total magnetization.

The time dependence of the transient reflectance, $\Delta R(t)/R$, for temperatures within Region I are displayed in Figure 3. In this region, when the sample consists of a majority of AF domains, a negative peak in the transient reflectance is detected, reaching a minimum value at a time delay of approximately 0.7 ps. Since this time delay is equivalent to the full width half maximum (FWHM) of the temporal correlation of our setup, we conclude that the rise time of this peak is on the sub-picosecond timescale. Additionally, the fall time of this peak does not exhibit a noticeable dependence on temperature.

At the onset of the AF/FM transition region (Region II and III) when the sample exhibits a mixed phase, the transient signal which is characteristic of the AF phase is observed. The $\Delta R(t)/R$ for temperatures within these regions is displayed in Figure 4. The peak magnitude decreases as the base temperature of the sample increases. At the center of the transition region, the peak magnitude of $\Delta R(t)/R$ becomes positive and continues to increase as the base temperature is further increased (Figure 5).

In addition to the peak magnitude, the fall time of the transient signal also depends on temperature. At the onset of the AF/FM transition (Region II), the fall time of the peak is equivalent to that of the AF phase. However at higher base temperatures (Region III and Region IV), the fall time decreases with increasing sample base temperature. Moreover, as the base temperature of the sample reaches Region V, the fall time of the transient peak is no longer detected. Since the sample consists of a majority of FM domains in this region, we conclude that the absence of the transient signal is a feature of $\Delta R(t)/R$ of the FM domains of the sample. Similar behavior is observed for the $\Delta R(t)/R$ for decreasing temperatures (Regions V-VII). The dependence of the sign of $\Delta R(t)/R$ on the AF and FM phase, Region

I and Region V, suggests that $\Delta R(t)/R$ depends on AF/FM phase fraction.

In addition to the dependence of the magnitude of $\Delta R/R(t)$ on the phase of the material, the results of our measurements exhibit a dependence of the fall time of $\Delta R(t)/R$ on the relative number of AF and FM domains in the sample.

IV. PHENOMENOLOGICAL MODEL

Using the temperature dependence of $\Delta R/R(t)$, we modelled the response of the system to pump pulse excitation prior to electron thermalization, using linear system techniques. In order to develop this model, we used the general processes exhibited by metals following excitation by an optical pump pulse.

In metals, it has been demonstrated that upon excitation by an optical pump pulse, hot electrons are excited above the Fermi energy.³¹ As a result, the electron distribution can no longer be described using Fermi-Dirac statistics. As time progresses, the hot electrons lose energy through electron-electron scattering until thermal equilibrium is reached with the electrons near the Fermi surface.

Shortly following the thermalization time of the electron distribution, the hot electrons diffuse through the sample where they lose energy by scattering with phonons in the lattice. These electron-phonon scattering events raise the temperature of the lattice until the electrons and phonons reach thermal equilibrium. After thermalization is achieved, electrons diffuse from the surface toward the substrate.³²

In this paper, we focused on the response of the sample to pump excitation prior to the thermalization of the electrons of the excited region. Since the temperature excursions induced by the optical pump pulses were 1% of the base temperatures of the sample, we were able to model the system using linear systems techniques.

To model the system at time delays shortly following excitation by the pump pulse ($t_{\text{delay}} \approx 1\text{-}2$ ps), the system response, $g(t)$, was determined using the convolution of the pump-probe correlation function, $C_{\text{pp}}(t)$, and the impulse response of the system, $h(t)$. This can be written as an expression of the following form,

$$g(t) = Q \times C_{\text{pp}}(t) * h_1(t), \tag{1}$$

where $Q = \sqrt{S_{2p} \times G}$. S_{2p} is the two-photon quantum efficiency and G is the impedance gain of the detector.³³ The time dependence of the system response was modeled using a decaying exponential,

$$h(t) = a(T)e^{-t/\tau_e(T)}, \quad (2)$$

where $\tau_e(T)$ is a phenomenological constant dependent on the thermalization time of the electrons of the system and $a(T)$ is a parameter that is dependent on the temperature dependent AF/FM phase fraction. The fitted time dependence of the transient reflectance ($\Delta R/R(t)$) are displayed in Figure 6

We determined the temperature dependence of $a(T)$ using the $\Delta R(t)/R$ for time delays less than and equal to 1 ps. We determined the FM phase fraction, $\Phi_{FM}(T)$, using the temperature dependence of $\Delta R(t_d=1 \text{ ps})/R$. Comparing these results with the temperature dependence of the magnetization determined using an MPMS, we found a similar temperature dependence. This comparison is shown in Figure 2. As a result, we conclude that the response of $\Delta R(t)/R$ at time delays larger than 1 ps is characteristic of the equilibrium AF/FM phase fraction determined using an MPMS. These results can be explained by the small pump fluence used during these measurements ($\approx 0.1 \text{ mJ/cm}^2$).

To determine $\tau_e(T)$ at a given base temperature, T , we used nonlinear least squares fitting to fit $g(t)$ to $\Delta R(t)/R$. The temperature dependence of $\tau_e(T)$ is displayed in Figure 7. Since the duration of the non-equilibrium response in the FM phase is shorter than the time resolution limit of our system, we only included temperatures where the majority of the probed region consists of AF domains. From this analysis, we conclude that for increasing temperatures where the probed region consists of a majority of AF domains, $\tau_e(T)$ decreases as the number of FM domains increases with temperature.

V. DISCUSSION

The phase-sensitivity of the two-tint time-domain thermorefectance on FeRh samples can be explained using the spin-polarized DOS for the AF and FM phases of FeRh that were referenced earlier.^{12,34} We will refer to these calculations to describe the wavelength dependence of these results. For the transient reflectance measurement, electrons are excited by the pump pulse to energies as high as 1.5 eV above the Fermi energy. Using the two-tint

measurement, where the combined bandwidth of the pump and probe pulse is approximately 10 nm, the probe pulse energy is also approximately 1.5 eV above the Fermi energy. As a result, electrons excited by the probe pulse also have energies approximately as high as 1.5 eV above the Fermi energy.

In the FM phase, shortly following excitation by the pump pulse, the probe pulse does not excite electrons due to Pauli blocking. Thus, there is not a drop in the transient reflectance. However in the AF phase, the total DOS at the probe pulse energy is approximately two times larger than in the FM phase. As a result, electrons are excited by the probe pulse in this phase. Consequently, the photons are absorbed and the transient reflectance decreases. Therefore, the sign difference of the transient reflectance of the AF and FM phases can be explained using the probe pulse wavelength and the electronic bandstructure.

Since the bandstructure of the AF and FM phase depends strongly on energy, this explanation of the reported results suggests that the transient reflectance of the AF and FM could also depend strongly on the wavelength of the probe pulse. This interpretation of these results is supported by the absence of this phase-dependence in the transient reflectance measurements using an 800 nm pump pulse and a 400 nm probe pulse. It is important to note that the explanation of these data was deduced using the experimental results presented.

The dependence of the electron thermalization time, $\tau_e(T)$, on temperature and phase fraction can be explained by the difference in the DOS of the AF and FM phases near the Fermi energy.¹⁸ Since the electron thermalization time is inversely related to the DOS at the Fermi energy, the electron thermalization time decreases as the DOS increases.¹⁹ Therefore, the electron thermalization time decreases as the FM phase grows in size. Using the experimental results of this study we have deduced that the electronic bandstructure has a dramatic effect on the equilibration time. Although this result is supported by theoretical calculations, this point is worthy of further experimental study.¹⁹

VI. CONCLUSIONS

We have used two-tint TDTR analysis to study the behavior of FeRh following pump pulse excitation. For these measurements, we used small temperature excursions to excite the system. We observed the response of the system at sample base temperatures below, above,

and throughout the AF/FM transition region. Our results show that the transient reflectance is sensitive to the AF and FM phase fraction. Using this phase-sensitive technique, our results indicate that in the low temperature region, the AF phase exhibits a large transient response to the pump pulse excitation. This response was not observed at temperatures above the AF/FM transition region, when the majority of the sample was ferromagnetic. In order to study the dependence of this transient response on the base temperature of the sample, we used linear system techniques to model the behavior of the system.

For this model, we represented the impulse response of the system using a decaying exponential function with a time constant representing the thermalization of the electrons of the system. Using this analysis, we determined that the thermalization of the electrons of the system in the AF phase occurred on a timescale approximately twice as long as that observed in the FM phase. This difference in timescale was explained using the results of electronic bandstructure calculations. In both the AF and FM phases, the time constant did not significantly depend on the base temperature of the sample. However within the AF/FM transition region, we observed that the thermalization time decreased as the fraction of FM domains increased. These results highlight the dependence of the electron thermalization time on AF/FM phase fraction.

In addition, the results of this study demonstrate the tunability of the sign of the transient reflectance using the electronic bandstructure of the material. Although the AF phase is difficult to probe in the presence of FM domains, these results demonstrate a method for detecting the AF phase at temperatures when the FM phase is present. Using the electronic bandstructure of FeRh, the AF and FM phases can be distinguished by tuning the wavelength of the pump and probe pulses. These results are significant, because they demonstrate the flexibility of TDTR to study the ultrafast response of materials which may otherwise be challenging to probe.

ACKNOWLEDGMENTS

The TDTR data collection, characterization and analysis for this project was conducted at the University of Illinois at Urbana-Champaign (UIUC) using the Materials Research Lab facilities while R. M. H. was a member of the research groups of Prof. David G. Cahill and Prof. Nadya Mason, whom we thank for guidance, fruitful discussions and support. This

effort was completed by R. M. H. in the group of Prof. Thomas A. Searles supported by the National Science Foundation through the University of Illinois at Urbana-Champaign Materials Research Science and Engineering Center DMR-1720633 and in part by the U.S. National Science Foundation CAREER Award DMR-2047905. In addition, F. H. and A.C. would like to acknowledge support from the Director, Office of Science, Office of Science, Office of Basic Energy Sciences, Materials Sciences and Engineering Division, U.S. Department of Energy, under Contract No. DE-AC02-05-CH11231 within the Nonequilibrium Magnetic Materials Program (KC2204), which supported the growth and magnetic characterization of the materials studied in this paper. Further, additional support came from NSF DMR MRSEC and the Illinois Fellowship.

- [1] L. H. Lewis, C. H. Marrows, and S. Langridge, Coupled magnetic, structural, and electronic phase transitions in FeRh, *Journal of Physics D: Applied Physics* **49**, 323002 (2016).
- [2] M. Fallot, Les alliages du fer avec les métaux de la famille du platine, *Annales de physique* **11**, 291 (1938).
- [3] P. A. Algarabel, M. R. Ibarra, C. Marquina, A. del Moral, J. Galibert, M. Iqbal, and S. Askenazy, Giant room-temperature magnetoresistance in the FeRh alloy, *Applied Physics Letters* **66**, 3061 (1995).
- [4] M. R. Ibarra and P. A. Algarabel, Giant volume magnetostriction in the FeRh alloy, *Physical Review B* **50**, 4196 (1994).
- [5] J.-U. Thiele, S. Maat, and E. E. Fullerton, FeRh/FePt exchange spring films for thermally assisted magnetic recording media, *Applied Physics Letters* **82**, 2859 (2003).
- [6] P.-W. Huang and R. H. Victora, Approaching the Grain-Size Limit for Jitter Using FeRh/FePt in Heat-Assisted Magnetic Recording, *IEEE Transactions on Magnetics* **50**, 1 (2014).
- [7] K. M. Cher, T. J. Zhou, and J. S. Chen, Compositional Effects on the Structure and Phase Transition of Epitaxial FeRh Thin Films, *IEEE Transactions on Magnetics* **47**, 4033 (2011).
- [8] A. Ceballos, Z. Chen, O. Schneider, C. Bordel, L.-W. Wang, and F. Hellman, Effect of strain and thickness on the transition temperature of epitaxial FeRh thin-films, *Applied Physics Letters* **111**, 172401 (2017).

- [9] C. Baldasseroni, C. Bordel, C. Antonakos, A. Scholl, K. H. Stone, J. B. Kortright, and F. Hellman, Temperature-driven growth of antiferromagnetic domains in thin-film FeRh, *Journal of Physics: Condensed Matter* **27**, 256001 (2015).
- [10] D. J. Keavney, Y. Choi, M. V. Holt, V. Uhlíř, D. Arena, E. E. Fullerton, P. J. Ryan, and J.-W. Kim, Phase Coexistence and Kinetic Arrest in the Magnetostructural Transition of the Ordered Alloy FeRh, *Scientific Reports* **8**, 1778 (2018).
- [11] L. J. Swartzendruber, The FeRh (Iron-Rhodium) system, *Bulletin of Alloy Phase Diagrams* **5**, 456 (1984).
- [12] S. P. Bennett, M. Currie, O. M. J. van 't Erve, and I. I. Mazin, Spectral reflectivity crossover at the metamagnetic transition in FeRh thin films, *Optical Materials Express* **9**, 2870 (2019).
- [13] M. A. de Vries, M. Loving, A. P. Mihai, L. H. Lewis, D. Heiman, and C. H. Marrows, Hall-effect characterization of the metamagnetic transition in FeRh, *New Journal of Physics* **15**, 013008 (2013).
- [14] F. Pressacco, V. Uhlíř, M. Gatti, A. Nicolaou, A. Bendounan, J. A. Arregi, S. K. K. Patel, E. E. Fullerton, D. Krizmancic, and F. Sirotti, Laser induced phase transition in epitaxial FeRh layers studied by pump-probe valence band photoemission, *Structural Dynamics* **5**, 034501 (2018).
- [15] G. Ju, J. Hohlfeld, B. Bergman, R. J. M. van de Veerdonk, O. N. Mryasov, J.-Y. Kim, X. Wu, D. Weller, and B. Koopmans, Ultrafast Generation of Ferromagnetic Order via a Laser-Induced Phase Transformation in FeRh Thin Films, *Physical Review Letters* **93**, 197403 (2004).
- [16] J.-U. Thiele, M. Buess, and C. H. Back, Spin dynamics of the antiferromagnetic-to-ferromagnetic phase transition in FeRh on a sub-picosecond time scale, *Applied Physics Letters* **85**, 2857 (2004).
- [17] S. O. Mariager, F. Pressacco, G. Ingold, A. Caviezel, E. Mohr-Vorobeva, P. Beaud, S. L. Johnson, C. J. Milne, E. Mancini, S. Moyerman, E. E. Fullerton, R. Feidenhans'l, C. H. Back, and C. Quitmann, Structural and Magnetic Dynamics of a Laser Induced Phase Transition in FeRh, *Physical Review Letters* **108**, 087201 (2012).
- [18] B. Bergman, G. Ju, J. Hohlfeld, R. J. M. van de Veerdonk, J.-Y. Kim, X. Wu, D. Weller, and B. Koopmans, Identifying growth mechanisms for laser-induced magnetization in FeRh, *Physical Review B* **73**, 060407(R) (2006).
- [19] B. Y. Mueller and B. Rethfeld, Relaxation dynamics in laser-excited metals under nonequilibrium conditions, *Physical Review B* **87**, 035139 (2013).

- [20] C. Yu, H. Li, Y. Luo, L. Zhu, Z. Qian, and T. Zhou, Thickness-dependent magnetic order and phase-transition dynamics in epitaxial Fe-rich FeRh thin films, *Physics Letters A* **383**, 2424 (2019).
- [21] K. Yang, K. Kang, Z. Diao, A. Ramanathan, M. H. Karigerasi, D. P. Shoemaker, A. Schleife, and D. G. Cahill, Magneto-optic response of the metallic antiferromagnet Fe₂As to ultrafast temperature excursions, *Physical Review Materials* **3**, 124408 (2019).
- [22] J.-U. Thiele, S. Maat, J. Robertson, and E. Fullerton, Magnetic and Structural Properties of FePt–FeRh Exchange Spring Films for Thermally Assisted Magnetic Recording Media, *IEEE Transactions on Magnetics* **40**, 2537 (2004).
- [23] B. T. Diroll, S. Saha, V. M. Shalaev, A. Boltasseva, and R. D. Schaller, Broadband Ultrafast Dynamics of Refractory Metals: TiN and ZrN, *Advanced Optical Materials* **8**, 2000652 (2020).
- [24] S. Maat, J.-U. Thiele, and E. E. Fullerton, Temperature and field hysteresis of the antiferromagnetic-to-ferromagnetic phase transition in epitaxial FeRh films, *Physical Review B* **72**, 214432 (2005).
- [25] K. Kang, Y. K. Koh, C. Chiritescu, X. Zheng, and D. G. Cahill, Two-tint pump-probe measurements using a femtosecond laser oscillator and sharp-edged optical filters, *Review of Scientific Instruments* **79**, 114901 (2008).
- [26] P. Jiang, X. Qian, and R. Yang, Tutorial: Time-domain thermoreflectance (TDTR) for thermal property characterization of bulk and thin film materials, *Journal of Applied Physics* **124**, 161103 (2018).
- [27] C. Baldasseroni, C. Bordel, A. X. Gray, A. M. Kaiser, F. Kronast, J. Herrero-Albillos, C. M. Schneider, C. S. Fadley, and F. Hellman, Temperature-driven nucleation of ferromagnetic domains in FeRh thin films, *Applied Physics Letters* **100**, 262401 (2012).
- [28] P. Drózdź, M. Ślęzak, K. Matlak, K. Freindl, N. Spiridis, D. Wilgocka-Ślęzak, A. Kozioł-Rachwał, J. Korecki, and T. Ślęzak, Perpendicular magnetic anisotropy and residual magnetic phases in gold-capped FeRh film on MgO(0 0 1), *Journal of Magnetism and Magnetic Materials* **495**, 165804 (2020).
- [29] W. Lu, P. Huang, K. Li, and B. Yan, Effect of substrate temperature on the crystallographic structure and first-order magnetic phase transition of FeRh thin films, *Journal of Materials Research* **28**, 1042 (2013).

- [30] R. Fan, C. J. Kinane, T. R. Charlton, R. Dorner, M. Ali, M. A. de Vries, R. M. D. Brydson, C. H. Marrows, B. J. Hickey, D. A. Arena, B. K. Tanner, G. Nisbet, and S. Langridge, Ferromagnetism at the interfaces of antiferromagnetic FeRh epilayers, *Physical Review B* **82**, 184418 (2010).
- [31] J. Stöhr and H. C. Siegmann, *Magnetism: from fundamentals to nanoscale dynamics*, Springer series in solid-state sciences No. 152 (Springer, Berlin ; New York, 2006) oCLC: ocm72867752.
- [32] J. Hohlfeld, S.-S. Wellershoff, J. Güdde, U. Conrad, V. Jähnke, and E. Matthias, Electron and lattice dynamics following optical excitation of metals, *Chemical Physics* **251**, 237 (2000).
- [33] S.-I. Shin and Y.-S. Lim, Simple Autocorrelation Measurement by Using a GaP Photoconductive Detector, *Journal of the Optical Society of Korea* **20**, 435 (2016).
- [34] M. E. Gruner, E. Hoffmann, and P. Entel, Instability of the rhodium magnetic moment as the origin of the metamagnetic phase transition in α -FeRh, *Physical Review B* **67**, 064415 (2003).

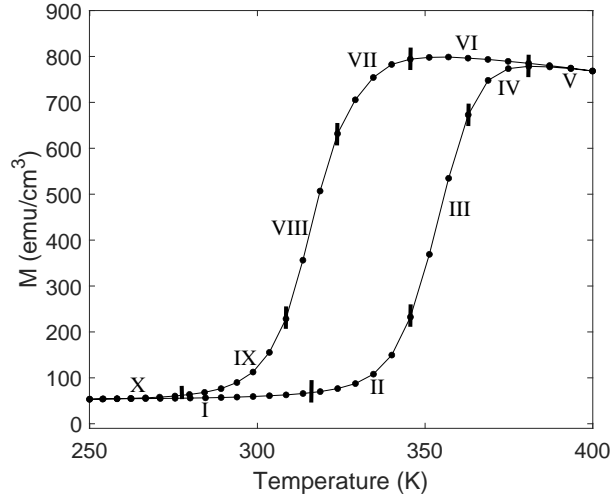


FIG. 1. **Temperature-dependent magnetization measurements of the Pt(3 nm)/FeRh(19nm)/MgO sample with an applied magnetic field of 900 Oe.** Temperature hysteresis is observed as follows. In regions I and V, the majority of the sample consists of antiferromagnetic (AF) domains for region I or ferromagnetic (FM) domains for region V. In Region I and X, there is a remnant ferromagnetic phase with a magnetization of approximately 59 emu/cm^3 . In regions II, III, and IV (VII, VIII, and IX) the sample undergoes the AF/FM transition for increasing (decreasing) temperatures. Differences in slope highlight different AF/FM transition mechanisms.

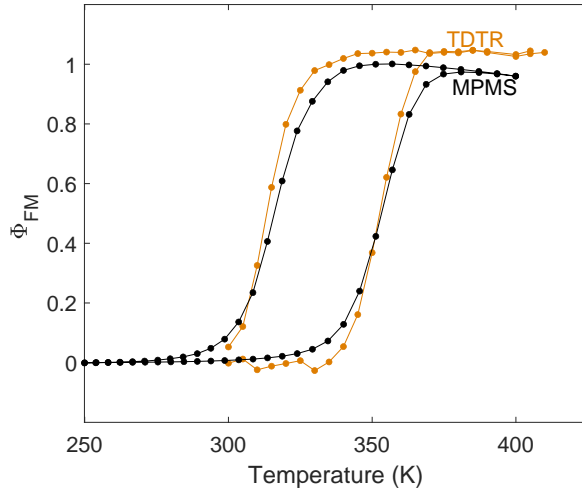


FIG. 2. Temperature dependence of the hysteresis of FM phase fraction (Φ_{FM}) determined using $\Delta R(t_d=1 \text{ ps})/R$ and SQUID magnetometry. The overlap of the TDTR and MPMS data suggest that for a given base temperature the FM phase fraction at $t_d=1 \text{ ps}$ is effectively equivalent to the equilibrium phase fraction at the base temperature.

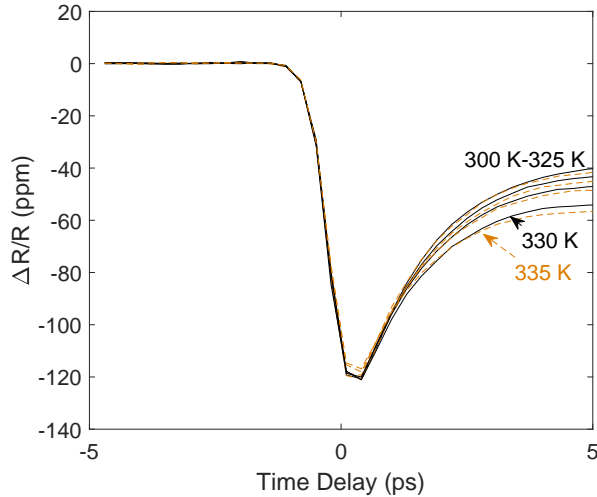


FIG. 3. Time dependence of the transient reflectance ($\Delta R(t)/R$) for temperatures within Region I ($T=300 \text{ K}-335 \text{ K}$). The transient reflectance does not exhibit a dependence on temperature within Region I. These results suggest that the nonequilibrium response is a characteristic of the AF phase and not due to thickness of the sample.

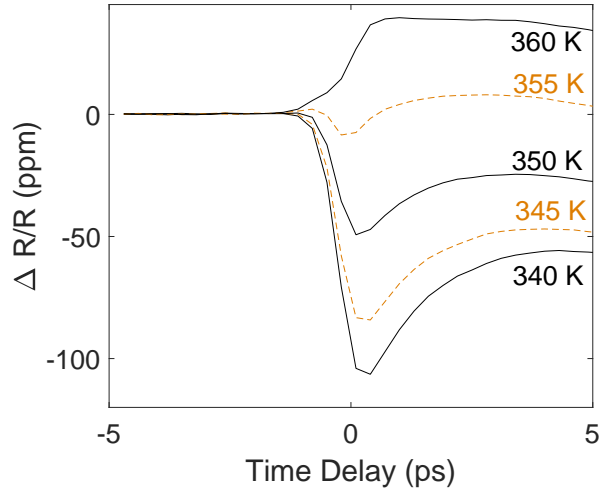


FIG. 4. Time dependence of the transient reflectance of the sample in the AF/FM transition region (Region III). In the transition region, $\Delta R(t)/R$ exhibits a negative peak shortly following pump excitation, that decreases in magnitude as the temperature is increased.

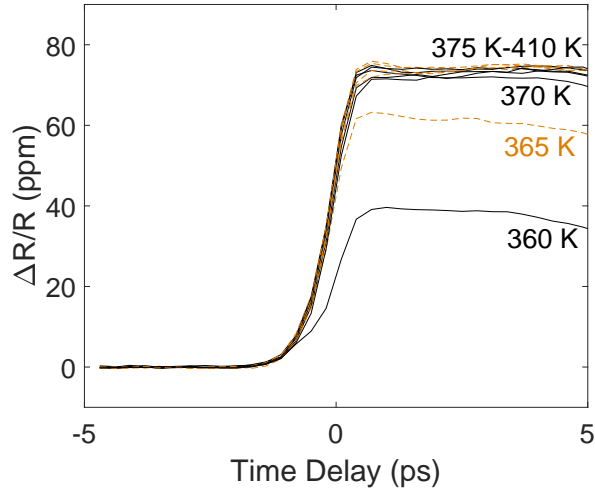


FIG. 5. Time dependence of the transient reflectance ($\Delta R(t)/R$) of the sample in the majority FM phase. In the FM phase, the time dependence of $\Delta R(t)/R$ does not depend on the base temperature of the sample. In addition, the transient response of the AF phase is not observed in the FM phase. Therefore, the FM domains do not exhibit a significant nonequilibrium response.

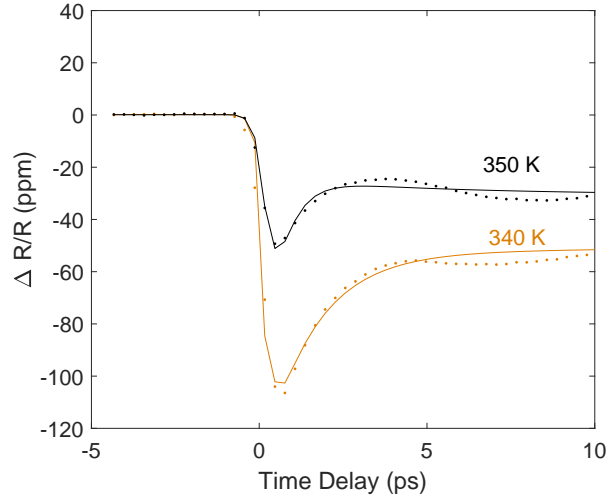


FIG. 6. **Fitted time dependence of the transient reflectance ($\Delta R/R(t)$) for temperatures in Region III.** The measured data is represented by solid dots and the fit is depicted by the solid line. The function used for the fit was $C_{pp}(t) \cdot a \times \exp^{-t/\tau_e} + b(t)$, where C_{pp} is the pump-probe correlation function and τ_e is a phenomenological constant representing the electron thermalization time. The parameters a and τ_e were used as free parameters. The function $b(t)$ is added to account for processes that occur after the thermalization of the electrons, phonons and magnons of the system.

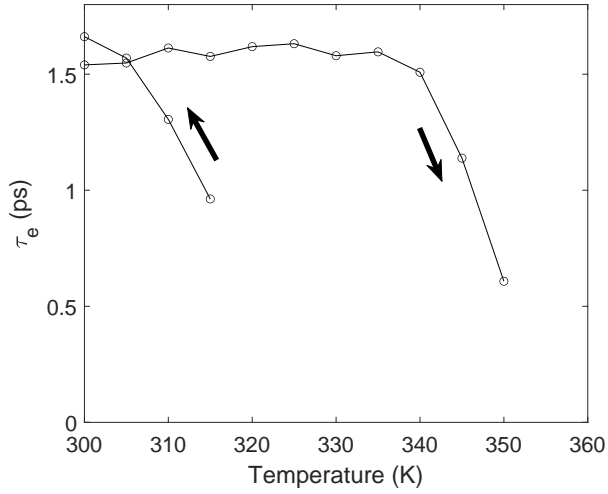


FIG. 7. **Temperature Dependence of τ_e .** In the low temperature region, when the sample exhibits a majority AF phase, τ_e is effectively constant. In the nucleation phase of the AF/FM transition region, τ_e decreases as the number of FM domains increases with the base temperature of the sample. In the domain-growth regime, where the FM domains grow in size, τ_e continues to decrease approaching the resolution limit of the TDTR system, 0.6 ps. When the sample consists of majority FM domains, τ_e reaches the resolution limit of the system. In the figure, the resolution limit of the TDTR setup is represented by a dotted horizontal line. For decreasing temperatures, τ_e increases and also exhibits hysteresis.